Biochimica et Biophysica Acta 1847 (2015) 486–492

Contents lists available at ScienceDirect

Biochimica et Biophysica Acta

journal homepage: www.elsevier.com/locate/bbabio

Identification of common motifs in the regulation of light harvesting: The case of cyanobacteria IsiA

Md. Wahadoszamen [a,b,*], Sandrine D'Haene [a], Anjue Mane Ara [a,c], Elisabet Romero [a], Jan P. Dekker [a], Rienk van Grondelle [a], Rudi Berera [a,1,**]

[a] Biophysics of Photosynthesis/Physics of Energy, Department of Physics Astronomy, Faculty of Sciences, VU University Amsterdam, The Netherlands
[b] Department of Physics, University of Dhaka, Dhaka 1000, Bangladesh
[c] Department of Physics, Jagannath University, Dhaka 1100, Bangladesh

ARTICLE INFO

Article history:
Received 16 July 2014
Received in revised form 27 November 2014
Accepted 12 January 2015
Available online 21 January 2015

Keywords:
Cyanobacteria
IsiA complex
Light-harvesting antenna
Photoprotective energy dissipation
Charge transfer states
Stark spectroscopy

ABSTRACT

When cyanobacteria are grown under iron-limited or other oxidative stress conditions the iron stress inducible pigment–protein IsiA is synthesized in variable amounts. IsiA accumulates in aggregates inside the photosynthetic membrane that strongly dissipate chlorophyll excited state energy. In this paper we applied Stark fluorescence (SF) spectroscopy at 77 K to IsiA aggregates to gain insight into the nature of the emitting and energy dissipating state(s). Our study shows that two emitting states are present in the system, one emitting at 684 nm and the other emitting at about 730 nm. The new 730 nm state exhibits strongly reduced fluorescence (F) together with a large charge transfer character. We discuss these findings in the light of the energy dissipation mechanisms involved in the regulation of photosynthesis in plants, cyanobacteria and diatoms. Our results suggest that photosynthetic organisms have adopted common mechanisms to cope with the deleterious effects of excess light under unfavorable growth conditions.

© 2015 Elsevier B.V. All rights reserved.

1. Introduction

Considered as the progenitor of the chloroplast, cyanobacteria appeared on Earth about 3.5 billion years ago and have marked the beginning of the conversion of a reducing atmosphere into an oxygen-rich oxidizing one. Cyanobacteria can inhabit almost every conceivable environment and their presence has been recorded from environments as diverse and harsh as hypersaline lakes, deep underneath the ocean, bare rocks and deserts. The robustness and tremendous adaptation capacity of cyanobacteria stem from a number of regulatory mechanisms that allow them to cope and thrive in the most different and inhospitable environments [1]. Since iron is an essential constituent for the synthesis of crucial proteins of the photosynthetic apparatus, the lack of iron imposes a severe impact on the overall photosynthetic activity of cyanobacteria. Despite being the most abundant element on Earth, the biological availability of iron for aquatic photoautotrophs like many cyanobacteria is limited because of its low solubility in aerobic ecosystems. Therefore, cyanobacteria very often face severe iron deficiency. To cope with it, the survival strategy of cyanobacteria evolved a variety of structural and functional changes. Under iron deficiency, the phycobiliprotein content and photosystem I (PSI) to photosystem II (PSII) ratio are typically reduced [2–4]. To compensate for this, some cyanobacteria express the iron stress induced *IsiAB* operon, which encodes for the synthesis of two proteins, IsiA and IsiB [5,6]. IsiB is a flavodoxin, which replaces the iron-rich soluble electron transfer protein ferredoxin [7,8]. IsiA belongs to the core complex family of chlorophyll a (Chl a)–carotenoid (Car) binding proteins and displays sequence homology with CP43, a core antenna protein of PSII [9,10]. IsiA is hence also referred to as CP43′. On average an IsiA monomer contains ~16 Chls a, 2 molecules of β-carotene, one molecule of zeaxanthin and one of echinenone [11]. IsiA was shown to form rings around the PSI reaction center thus forming a supercomplex consisting of a trimeric or monomeric PSI and up to 18 IsiA subunits [12,13] in a first ring and up to 25 in a second one [14]. IsiA supercomplexes, obtained from *Synechocystis* sp. PCC 6803 grown under variable degree of iron depletion, revealed that IsiA can also form other types of rings (or fractions of rings) devoid of PSI and having a variable number of IsiA subunits [14,15]. The oligomeric IsiA surrounding PSI was shown to increase the effective absorption cross-section thus acting as an auxiliary light-harvesting antenna during iron starvation [16]. In the 18-unit ring structure, the light-harvesting capacity of the IsiA–PSI complex was found to be almost

* Corresponding author at: Biophysics of Photosynthesis/Physics of Energy, Department of Physics Astronomy, Faculty of Sciences, VU University Amsterdam, The Netherlands. Tel.: +31 20 59 87426; fax: +31 20 59 87999.
** Corresponding author. Tel.: +31 20 59 87426; fax: +31 20 59 87999.
E-mail addresses: m.d.wahadoszamen@vu.nl (M. Wahadoszamen), r.berera@vu.nl (R. Berera).
[1] Present address: The OCU Advanced Research Institute for Natural Science and Technology (OCARINA), Osaka City University, Sugimoto, Sumiyoshi-ku, Osaka 558-8585, Japan.

http://dx.doi.org/10.1016/j.bbabio.2015.01.003
0005-2728/© 2015 Elsevier B.V. All rights reserved.

double compared to that of the PSI core [17,18]. Besides IsiA–PSI complexes, IsiA aggregates completely devoid of the central PSI subunit can also be formed at the early stages of iron depletion and their synthesis is increased under prolonged stress [19]. These complexes are strongly quenched and thus suggested to be responsible for photoprotective thermal dissipation of excess energy [11,20–22]. More light in favor of the photoprotective role of IsiA was provided by Havaux and co-workers [23] who showed that the genetic expression of IsiA can be triggered by high light. The IsiA gene is also expressed when the organism is exposed to oxidative stress, high ionic strength and heat [24,25]. Unlike the main light-harvesting complex (LHCII) of plants, which can switch from a light harvesting to an energy dissipating state [26], IsiA only exists in the quenched (aggregated) state. Therefore, IsiA performs two seemingly opposite physiological functions; it acts as light-harvesting antenna when connected to PSI and at the same time acts as an efficient energy dissipater when found in aggregates devoid of PSI.

A significant amount of work has been devoted over the last two decades to unravel the spectroscopic properties and structure-function relationship of IsiA. It has been proposed that IsiA and LHCII have adopted a common energy dissipation mechanism where a low-lying Car singlet state acts as energy sink [27] thus safely dissipating the (excess) energy as heat [22,28]. It has been proposed that the Car echinenone may act as a quencher in IsiA aggregates [22] since it is more efficient than the other Cars in transferring energy to neighboring Chls [29], suggesting a more favorable position to accept energy from neighboring excited Chl(s). By possessing a keto carbonyl group partly conjugated with its carbon–carbon backbone, echinenone also possesses an intramolecular charge transfer (ICT) state when bound to IsiA [29].

Energy dissipation in higher plants has been suggested to be regulated by both intermolecular and intramolecular charge transfer (CT) states [30–32]. Stark spectroscopy, which detects the electric field-induced changes in spectral intensity, is a very useful experimental technique for the investigation of the structure and dynamics of molecular or supramolecular systems, especially those having CT character [33–35]. It is also a sensitive technique to resolve individual spectra and study the structure and dynamics of molecular species which, because of having closely lying energy levels, yield a single spectral profile in conventional spectroscopy [32]. Recently we have successfully applied SF spectroscopy to LHCII of plants and to the fucoxanthin-chlorophyll proteins (FCPs) of diatoms in their dissipative states, where we detected two emitting sites characterized by spectrally very different responses to the electric field [32,36]. In the present study, we have applied the same technique to IsiA to look for the possible contributions of different species in the energy dissipation process.

2. Materials and methods

2.1. Samples preparation and analysis

IsiA samples were prepared from *Synechocystis* sp. PCC 6803 cells grown for 2–3 weeks in BG11 without iron, with constant stirring at 100 rpm, at light intensity of 50 μmol of photons m^{-2} s^{-1}, 25 °C and in ambient air. Wild type (WT) cells were used for preparations containing some PSI and *psaFJ-null* mutant of *Synechocystis* sp. PCC 6803 for IsiA aggregates without PSI. After centrifugation for 5 min at 7500 ×*g* the harvested cells were resuspended in mannitol buffer (0.25 mM mannitol, 50 mM Bis Tris pH 6.5, 10 mM NaCl, 5 mM KH_2PO_4, 5 mM K_2HPO_4) with addition of 1 mM benzamidine, 1 mM caproic acid, 1 mM EDTA and few milligrams of DNase (bovine pancreas type IV, Sigma) and then disrupted by French press at 11,000 psi (7.6 x 10^7 Pa). The thylakoid membranes were prepared by centrifugation at 500 ×*g*, 4 °C, for 5 min to separate the membranes from unbroken cells and by centrifugation at 13,000 ×*g*, 4 °C, for 5 min of the supernatant with resuspension in 25 mM Hepes pH 7.5, 20 mM NaCl buffer two times to remove phycobilisomes. IsiA was further isolated as previously described [11].

PSI was isolated by a 2-step purification of solubilized thylakoid membranes prepared as described here for IsiA preparations but this time from WT *Synechocystis* sp. PCC 6803 grown in complete BG11 medium. The thylakoids were solubilized with 10% (w/w) n-dodecyl-β-D-maltopyranoside (β-DDM) to a final concentration of 1% for 1 mg/ml of Chl a and by incubation at RT for 5 min with gentle mixing. After centrifugation for 3 min at 11,500 ×*g* the supernatant was separated from the pellet for injection into a Mono Q HR 10/10 column equilibrated with BTT buffer (20 mM Bis Tris pH 6.5, 10 mM $MgCl_2$, 20 mM NaCl, 10 mM $CaCl_2$, 1.5% taurine, 0.03% β-DDM). Unbound material was washed away at a flow of 0.5 ml/min increased to 0.8 ml/min within 5 min. Then a gradient of BTT buffer with $MgSO_4$ was applied at a flow of 0.5 ml/min in several steps (20 min to reach 50 mM $MgSO_4$, 10 min to 100 mM, 25 min to 250 mM). Next, gel filtration was performed on concentrated fractions (Amicon® Ultra Centrifugal Filter 10K device, Millipore) containing PSI with a Superdex 200 HR 10/30 column (Pharmacia) at a flow of 0.45 ml/min after equilibration with BTT buffer. The obtained PSI fractions were concentrated with an Amicon® Ultra 10K device (Millipore) for further use.

SDS–PAGE was carried out according to Laemmli [37] with some modifications. The samples were denatured with 6% (w/v) LDS, 50 mM DTT and by incubation at 37 °C for 30 min, then applied on a gel of 12% (v/v) acrylamide containing 2 M urea and 0.1% (w/v) SDS. PageRuler Prestained (Fermentas) was used as protein ladder. Proteins were visualized on the gel by Coomassie staining using a PageBlue Protein Staining solution (Thermo Scientific).

Immunoblot was performed against PsaA and PsbA (Agrisera) on a nitrocellulose Whatman membrane (Sigma-Aldrich) after transfer from the SDS–PAGE here described. A goat anti-rabbit IgG horse radish peroxidase (HRP) conjugated (Agrisera) was used as secondary antibody and the activity of the peroxidase was visualized with SuperSignal™ West Pico chemiluminescent substrate (Thermo Scientific). The membrane and the gel were imaged with the Luminescent Image Analyser ImageQuant LAS 4000 (GE Healthcare).

2.2. Stark sample preparation and SF data analysis

The samples were prepared by suspending them in a buffer containing 20 mM Bis Tris pH 6.5, 10 mM $MgCl_2$, 0.06% β-DDM (but without detergent for membranes preparations) and with glycerol at 60% (v/v) final concentration for SF spectroscopy measurement at 77 K in a cell and homebuilt setup, as earlier described [32,36]. The OD of IsiA at 670 nm measured through the Stark cell at 77 K was 0.25 at 670 nm and for PSI was 0.95 at 683 nm. The details about the analytical treatment of the obtained SF data can be found elsewhere in the literature [36,38]. According to the standard Liptay formalism, the SF intensity of randomly distributed and spatially fixed emitting chromophores having negligible (inter-chromophore) excitonic interactions can often be described as the weighted sum of the zeroth, first, and second derivatives of the F spectrum:

$$\frac{2\sqrt{2}\Delta F(\nu)}{F_{\max}} = (f\boldsymbol{F_{ext}})^2\left\{A_\chi F(\nu) + B_\chi \nu^3 \frac{d\left[F(\nu)/\nu^3\right]}{d\nu} + C_\chi \nu^3 \frac{d^2\left[F(\nu)/\nu^3\right]}{d\nu^2}\right\} \quad (1)$$

Where $F_{\max}$ is the maximum F intensity, $\boldsymbol{F_{ext}}$ is the amplitude of the externally applied electric field, χ is the experimental angle between the direction of $\boldsymbol{F_{ext}}$ and the electric polarization of the excitation light of energy ν, and f is the local field correction factor that relates $\boldsymbol{F_{ext}}$ with the internal electric field ($\boldsymbol{F_{int}}$) experienced by the chromophore ($\boldsymbol{F_{int}} = f\boldsymbol{F_{ext}}$). The weight of the zeroth derivative gives an estimate of the field-induced change in emission intensity arising mostly from field-induced modulation of the rates of the associated nonradiative deactivations. Besides, the weights of the first and the second derivatives often provide crucial information about the electronic structure, more

specifically changes in electrostatic parameters such as molecular polarizability ($\Delta\alpha$) and dipole moment ($\Delta\mu$) between the ground and excited states upon F transition, respectively [35,36,38]. At magic angle ($\chi = 54.7°$) the coefficients B_χ and C_χ can be expressed as [36,38]

$$B_{54.7°} = \frac{\Delta\alpha}{2hc} \tag{2}$$

$$C_{54.7°} = \frac{(\Delta\mu)^2}{6h^2c^2}. \tag{3}$$

Therefore, if the SF spectrum is fitted with a linear superposition of the derivatives of the respective F spectrum and the coefficients of the first and second derivatives are computed, one can extract the values of $\Delta\alpha$ and $\Delta\mu$ from the above two equations.

3. Results and discussion

Previous time-resolved emission measurements at 77 K showed that the emission of IsiA aggregates is very strongly quenched, with an average lifetime of less than 200 ps [19]. Performing SF spectroscopy at 77 K on IsiA aggregates then gives us the opportunity to analyze the Stark properties of a strongly quenched system at this temperature. The pronounced quenching also puts strong constraints on the quality of the sample, because small contaminations with long-living species such as free Chls or the red Chls in PSI can give large distortions of the recorded spectra. For this reason, the purity of the IsiA samples used for the Stark measurements was analyzed by SDS–PAGE (Fig. 1a) and immunoblot was performed against the PsaA sub-unit of PSI and PsbA of PSII (Fig. 1b). The PSI preparation (line 2 of Fig. 1a) was also loaded on SDS–PAGE yielding several bands of which the one with the highest molecular weight at 60 kDa corresponds to the sub-units PsaA and PsaB. Additional lower bands for the sub-unit PsaD, –F and –L with apparent molecular weight around 15 kDa were also obtained. Smaller subunits of PSI (PsaE, –C, –I, –J, –K and –M) were not resolved on a 12% acrylamide gel. The IsiA samples give a band around 27 kDa and contain no visible PSI band when isolated from *psaFJ-null* mutant, while for IsiA isolated from the WT, bands found in the PSI sample (PsaA, –B, –D, –F, –L) could be visualized (data not shown). To confirm our results we performed an immunoblot against PsaA and PsbA. In the PSI sample PsaA was detected but could not be visualized from the IsiA aggregates. To further test the purity of isolated PSI and IsiA aggregates, PsbA antibody was also used and a negative reaction was obtained in these preparations.

The upper and lower panels of Fig. 2 present the F and SF spectra at 77 K of isolated IsiA aggregates obtained from the *psaFJ-null* mutant of *Synechocystis* PCC 6803 cells grown under 18 days of iron starvation. The F and SF spectra of IsiA are denoted hereafter as F IsiA and SF IsiA, respectively. In addition to the biochemical analysis, spectroscopic comparison of this sample with other IsiA preparations containing variable amounts of PSI and subsequent SF analysis (as will be presented in Figs. 4 and 5) allowed us to rule out the presence of PSI contamination in the IsiA preparation presented in this manuscript. Both the F IsiA and SF IsiA signals are recorded simultaneously with an excitation wavelength of 441 nm where the sample has negligible Stark absorption (SA) signal (Fig. S1 of the ESI). The SF IsiA spectrum is scaled to the field strength of 1 MV cm^{-1}, although the actual field applied during the measurement has a magnitude within the range 0.35 to 0.49 MV cm^{-1}. The F IsiA exhibits a characteristic sharp and well defined emission band with a peak at 684 nm, accompanied by vibrational satellites in the longer wavelength region [11,19]. The SF IsiA on the other hand gives overall negative amplitude with a peak at 685 nm and with a shape very similar to that of the F spectrum. The spectral similarity indicates that the field-induced reduction (as revealed by the negative amplitude) of the F intensity is the dominant contribution to the SF spectrum. The intensity of SF IsiA was found to increase

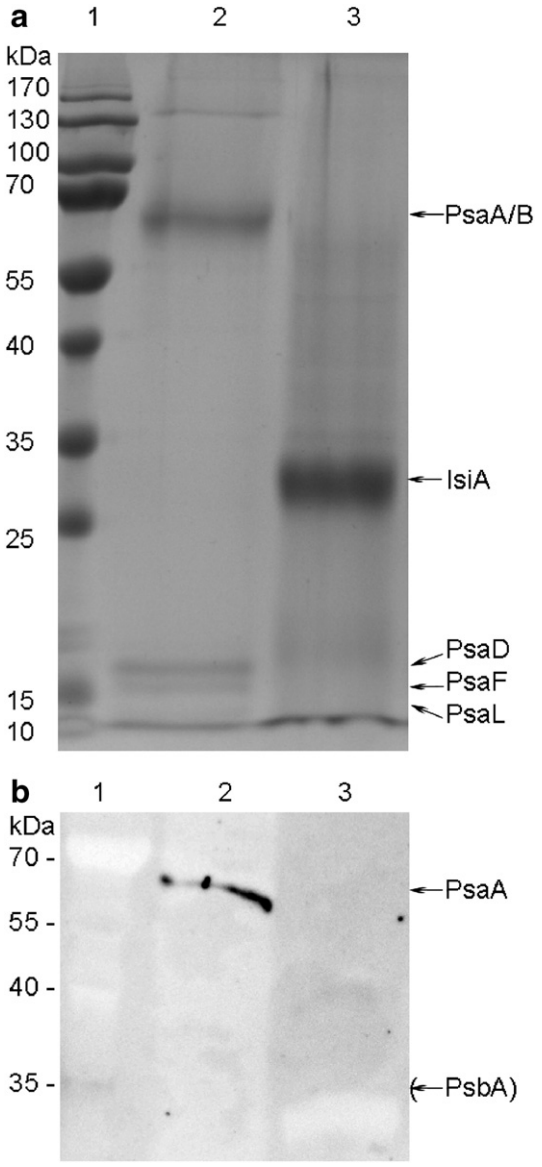

Fig. 1. Biochemical analysis with molecular weight markers (line 1), PSI preparation (line 2) and IsiA aggregates (line 3). (a) SDS–PAGE with all samples loaded at 1.3 μg of Chl. The band at around 60 kDa corresponds to PsaA and PsaB of PSI, the band at 27 kDa corresponds to IsiA and the lower bands to other PSI sub-units (PsaD, –F and –L). (b) Immunoblot using antibody against PsaA (band on line 2) and PsbA (which appears at 30 kDa if present) with 0.7 μg of Chl loaded per line on the gel for transfer.

quadratically upon increasing the magnitude of the applied electric field as expected for a homogenously distributed and spatially immobilized sample (inset of Fig. S2 of the ESI). However, if we carefully compare the shapes of the F and SF spectra, we see that they are not completely identical; more specifically, the shape of the SF IsiA around both the shorter (660–678 nm) and longer (720–750 nm) wavelength regions is rather different from that of the F spectrum.

To gain further insight, we modeled the SF IsiA by applying the standard Liptay formalism, by which the observed SF spectrum is fitted as a linear superposition of the zeroth, first and second derivatives of the F IsiA. The resulting fit is shown by the solid magenta line in Fig. 3a together with the SF spectrum (square-dotted red line). In essence, the zeroth derivative of the F IsiA gives the dominant contribution to the fitting with negative sign together with a small, but non-negligible contribution of both the first and second derivatives. The magnitude of the field-induced reduction of the F intensity (FIRFI), estimated from the coefficient of the zeroth derivative necessary for the fit, is evaluated to be

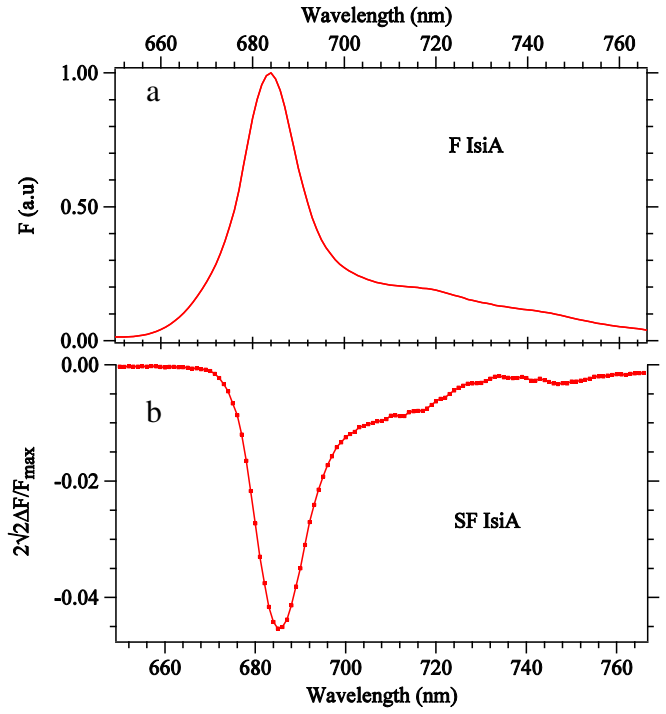

Fig. 2. (a) F and (b) SF spectra of IsiA recorded simultaneously at 77 K with an excitation wavelength of 441 nm. The SF spectrum is normalized to a field strength of 1 MV cm^{-1} and to the F intensity at the peak of the F spectrum.

about 4.2% at the field strength of 1 MV cm^{-1}. The magnitude of the change in molecular polarizability ($\Delta\alpha$) and dipole moment ($\Delta\mu$), extracted respectively from the coefficients of the first and second derivatives of the fit, is found to be −79 [$Å^3/f^2$] and 0.92 [D/*f*], respectively. As can be clearly seen in Fig. 3, this approach does not yield a satisfactory fit of the SF IsiA; in fact while in the 685 nm region the fit has a very good match with the SF spectrum, a clear mismatch is present both in the shorter (660–680 nm) and longer (720–765 nm) wavelength regions. This observation demonstrates that the 77 K SF signal for IsiA aggregates cannot be fitted by considering a single F band. Furthermore, the subtraction between the SF and the fit results in two distinct bands located in the 660–680 nm, and 715–765 nm wavelength regions, respectively (Fig. 3b, dSF IsiA). The shape of the 660–680 nm band is somewhat sharp and has a peak at around 672 nm. As far as the spectral position is concerned, this band is very likely to originate from some free Chls present in the IsiA preparation [11]. Since, like for photoactive monomeric tetraphenylporphyrin [39], free Chls are expected to give only a small contribution to the SF signal as can be judged from Fig. 3a, and thereby do not affect the signal in the red region, the contribution of free Chls will not be further discussed in the paper. On the other hand, the band around 715–765 nm is clear and rather broad with a peak at around 730 nm and a long tail extending up to ~765 nm. Thus, if we leave aside the signal originating from free Chls, the SF IsiA is characterized by a main band peaking at 685 nm and a putative new band with a peak at around 730 nm. Note that we also observed a similar long wavelength band from the analysis of the SF of different IsiA preparations (Fig. S3 of ESI), which indicates that the appearance of this band is reproducible. We can infer at least two possibilities about its origin. i) It may appear from a trace presence of PSI (which could not be detected by SDS–PAGE analysis) in IsiA since it is difficult to obtain

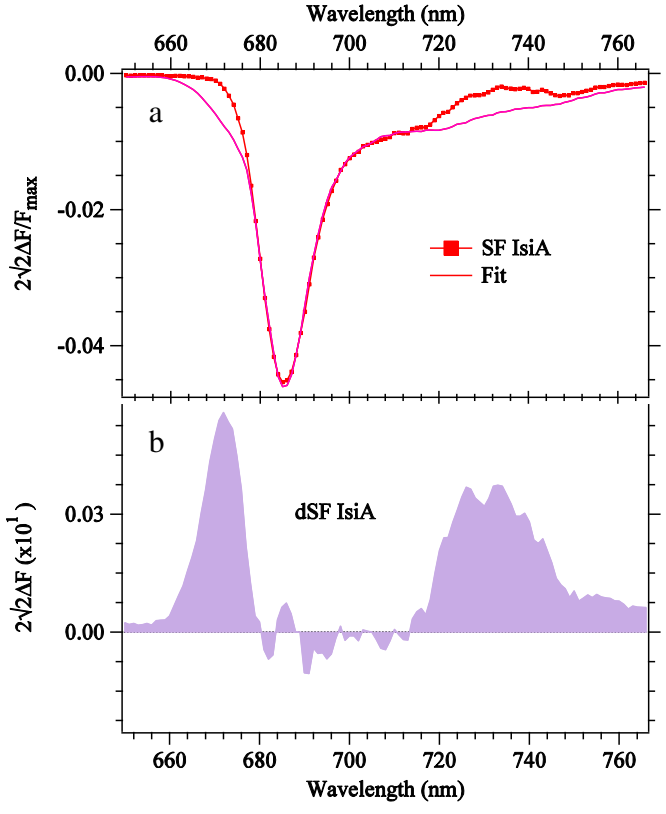

Fig. 3. (a) SF (square-dotted red line) spectrum of IsiA and the fit (magenta solid line) obtained with a linear superposition of the zeroth, first and second derivatives of the corresponding F spectrum (shown in Fig. 1a). (b) Result of the subtraction (dSF IsiA) between the SF spectrum and the fit.

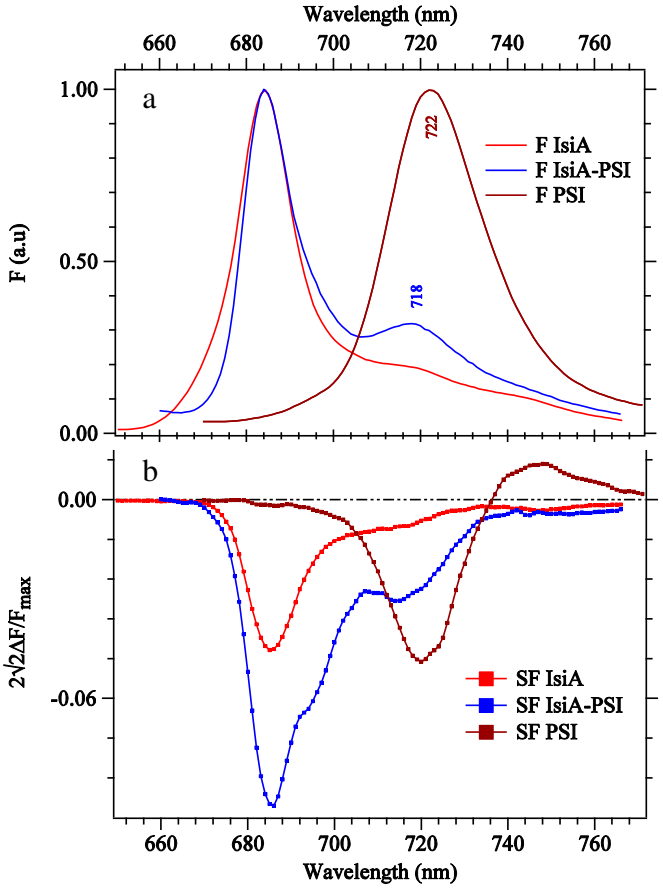

Fig. 4. (a)/(b) F/SF spectrum of IsiA (F IsiA/SF IsiA), IsiA–PSI (F IsiA–PSI/SF IsiA–PSI) and PSI (F PSI/SF PSI) recorded simultaneously at 77 K with an excitation wavelength of 441 nm.

IsiA completely devoid of PSI, and if PSI is present, the red Chls have high quantum yields compared to IsiA [40]. ii) It may appear from a new F species in IsiA, which cannot be distinguished in the F spectrum.

To further test the possibility of PSI involvement in the SF signal, we measured the SF spectra of an isolated PSI preparation and of a different IsiA sample containing a small percentage of PSI (IsiA–PSI). Fig. 4a and b display the F and SF spectra of isolated PSI and IsiA–PSI, respectively. For the sake of better comparison, the spectra of IsiA were also appended in this figure. One can easily notice that PSI, be it either in isolated form or in complex with IsiA, yielded apparently identical emission profile except for the position of the peak which is slightly (4 nm) blue shifted for the IsiA–PSI complex [16,19]. It is also evident that IsiA gives flat emission in the region where the IsiA–PSI complex exhibits a structured emission from PSI, confirming that if a small amount of PSI is present in the IsiA preparation, its effect on the IsiA emission spectrum is negligible. Isolated PSI yielded a derivative-like SF lineshape (SF PSI) with distinct negative and positive bands. However, like for IsiA, IsiA–PSI gave a SF signature (SF IsiA–PSI) whose amplitude is negative all through the selected spectral window. Although the amplitude is negative, one can easily recognize the structured signature of the PSI contribution in the SF IsiA–PSI (706–765 nm wavelength region) and a fairly resolved shallow SF lineshape in the 690–705 nm region. The shallow SF lineshape is likely to arise from some trace presence of PSII within the IsiA–PSI preparation and thus we will not focus our attention to this band hereafter.

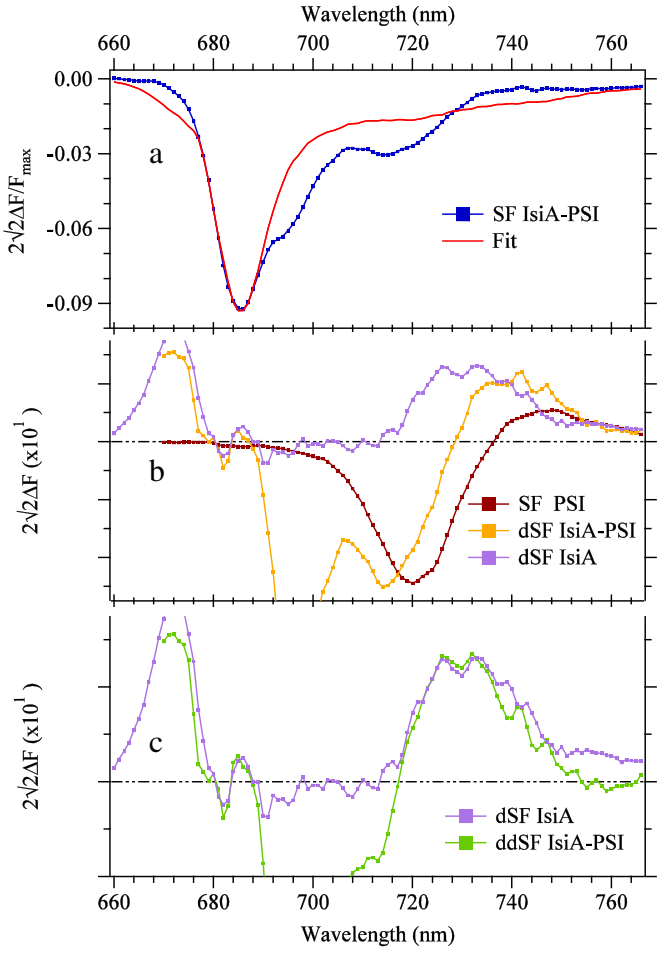

Fig. 5. (a) SF IsiA–PSI (square-dotted blue line) and the corresponding fit (red solid line) obtained with the derivative combination of the F IsiA spectrum. (b) Result of subtraction (dSF IsiA–PSI) (square-dotted orange line) between SF IsiA–PSI and the corresponding fit, SF PSI (square-dotted deep red line) and dSF IsiA (square-dotted light blue line). (c) Result of subtraction (ddSF IsiA–PSI) (square-dotted green line) between the normalized shapes of dSF IsiA–PSI and SF PSI, and dSF IsiA (square-dotted light blue line).

To isolate the PSI SF contribution from SF IsiA–PSI, we first modeled SF IsiA–PSI on the basis of the standard Liptay formalism. To this end, we used the emission lineshape of IsiA emission (F IsiA) which contains negligible contribution from PSI. Fig. 5a presents the SF IsiA–PSI (square-dotted blue line) together with the fit (solid red line) obtained with the weighted superposition of the derivatives of the IsiA F. The model yields a satisfactory fit in the IsiA emission region but shows a clear mismatch both in the shorter and longer wavelength regions. Again, the mismatch in the shorter wavelength region arises from contribution of free Chls in the emission lineshape of IsiA, whereas the one in the longer wavelength region comes from the interplay of both PSII and PSI present in the IsiA–PSI preparation. To extract the SF lineshape of PSI, the resulting fit was subtracted from SF IsiA–PSI. The subtraction yielded a derivative–like SF lineshape in the longer wavelength region (705–765 nm) which has a shape very similar to that of SF PSI. Fig. 5b presents the resulting difference (dSF IsiA–PSI) together with dSF IsiA and SF PSI. For the sake of a better comparison the intensity of the negative peaks of dSF IsiA–PSI (at 714 nm) and SF PSI (at 720 nm) is normalized and the dSF IsiA is amplified by a factor 2.5. One can easily notice that despite the overall shape of dSF IsiA–PSI around 705–765 nm is seemingly identical to SF PSI, it is shifted to the blue by about 8 nm and gives a much more pronounced positive band compared to the one of PSI SF. As mentioned earlier, the PSI of IsiA–PSI complex gives a 4 nm blue shifted emission compared to isolated PSI. Therefore, if the obtained derivative like lineshape around 705–765 nm of dSF IsiA–PSI signal originated solely from PSI, it would display the same extent of blue shift with respect to the SF of isolated PSI. The observed blue shift of 4 nm together with the relatively larger positive intensity thus point to the presence of other spectral species besides PSI in the dSF IsiA-PSI spectrum. To reveal the tentative spectral shape of the unknown species, we have carried out a subtraction between the normalized shapes of dSF IsiA–PSI and SF PSI shown in Fig. 5b. Fig. 5c displays the spectral profile (ddSF IsiA–PSI) resulted upon subtraction together with the shape of dSF IsiA. Interestingly, the resulting difference spectrum of ddSF IsiA–PSI gives a positive band peaking at 730 nm and has a shape similar to that of dSF IsiA in the 710–765 nm region (Fig. 3b). This suggests that the SF spectra of both IsiA and IsiA–PSI contain a contribution from a new putative species giving SF signature in the 730 nm region. As obtained upon separating the contribution of SF PSI from SF IsiA–PSI, we can conclude that the 730 nm SF signature of IsiA–PSI does not originate from PSI.

Therefore we assign the observed SF signal around 720–765 nm in the dSF IsiA (Fig. 3b) to a new band originating from IsiA emission. The new F species could not be detected in the F spectrum but could be separated from the main 684 nm band by the application of the electric field. The new species shows very different and strong response to the external electric field compared to the 684 nm band and PSI. The pronounced appearance in the SF spectrum in fact implies that, in analogy with electric field effects in other artificial donor-acceptor complexes [39,41], the new species possesses a considerably large CT character. However, the almost indistinguishable F feature of the red state does not allow us to accurately estimate the magnitude of its CT character from the present analysis. We have recently shown that two emitting states are present in the dissipative state of the main light-harvesting antenna of plants and diatoms, LHCII and FCPs respectively [32,36]. One state was assigned to a Chl–Chl CT state mixed with the lowest exciton state. The second state is characterized by a red-shifted SF signal peaking at 713–715 nm in LHCII and at 702–713 nm in FCPa. Detailed analyses showed that the corresponding F states of the red-shifted SF signals have very strong CT character. While for LHCII and FCPs the system can be prepared and studied in different energy dissipating states [32,36], this is not possible for aggregated IsiA, which is permanently in an energy dissipating state. If we compare the results we obtained for LHCII and FCPs with those for IsiA, we see that all

samples in the dissipative state show a main emission band and remarkably similar SF signature in the red region of the spectrum; the corresponding red fluorescent band is characterized by a very strong response to the electric field, but very weak emission intensity. In LHCII [32] and FCPs [36] we proposed that the red band originates from Chl–Car interaction. Likewise in IsiA this band may originate from the interaction between one or more Chl pigments and a Car molecule. Among the other Car species in the system, IsiA contains one echinenone molecule per monomer. By possessing a keto-carbonyl group partly conjugated with its carbon–carbon backbone this Car not only displays a CT character in the excited state, but the amount of CT character is very sensitive to the local environment both in solution [42] and when the Car is embedded in a protein [43]. In particular small changes in the protein environment have a pronounced effect on the CT character of the Car excited state [43,44]. Transient absorption studies on IsiA aggregates upon selective Chl excitation have shown that the quenching species, identified as a Car, shows broad excited state absorption, thus pointing to the presence of a CT state [22]. We have shown that echinenone in IsiA is more effective in transferring energy to Chls when compared to the other Car species in the system, β-carotene and zeaxanthin [29]. Even though more studies on IsiA with different carotenoid composition and possibly on monomeric IsiA are required to identify the quenching species, we suggest that the red band originates from the interaction between the echinenone S_1/ICT state and the lowest emissive Chl excitonic state of IsiA. This interaction may lead to an energy transfer mechanism where the Car ICT state of echinenone accepts energy from the excited Chl(s) and dissipates it as heat. A similar mechanism has recently been proposed to be responsible for phycobilisome fluorescence quenching in cyanobacteria [45] where the echinenone-binding orange carotenoid protein plays a key role in the process [46].

Acknowledgments

The authors thankfully acknowledge the contribution of Jos Thieme for his technical assistance. Md.W. was supported by the Netherlands Organization for Scientific Research (NWO) via a visitor grant. Md.W., E.R. and R.v.G. were further supported by NWO via a TOP-grant (700.58.305) from the Council of Chemical Sciences to R.v.G., an Advanced Investigator grant from the European Research Council (nr. 267333, PHOTPROT) to R.v.G. and by the Laserlab-Europe Consortium. E.R. and R.v.G. were also supported by the EU FP7 project PAPETS (GA 323901). R.B. was supported by the Earth and Life Sciences Council of the Netherlands Foundation for Scientific Research (NWO-ALW) through a Rubicon and Veni grants and via PHOTPROT.

Appendix A. Supplementary data

Supplementary data to this article can be found online at http://dx.doi.org/10.1016/j.bbabio.2015.01.003.

References

[1] A.R. Grossman, M.R. Schaefer, G.G. Chiang, J.L. Collier, The responses of cyanobacteria to environmental conditions: light and nutrients, in: D.A. Bryant (Ed.), The Molecular Biology of Cyanobacteria, Kluwer Academic Publishers, Dordrecht, The Netherlands, 1994, pp. 641–675.
[2] G. Sandmann, R. Malkin, Iron–sulfur centers and activities of the photosynthetic electron-transport chain in iron-deficient cultures of the blue–green-alga *Aphanocapsa*, Plant Physiol. 73 (1983) 724–728.
[3] G. Sandmann, Consequences of iron-deficiency on photosynthetic and respiratory electron-transport in blue–green-algae, Photosynth. Res. 6 (1985) 261–271.
[4] J.A. Guikema, L.A. Sherman, Organization and function of chlorophyll in membranes of cyanobacteria during iron starvation, Plant Physiol. 73 (1983) 250–256.
[5] D.E. Laudenbach, N.A. Straus, Characterization of a cyanobacterial iron stress-induced gene similar to *psbC*, J. Bacteriol. 170 (1988) 5018–5026.
[6] D.E. Laudenbach, M.E. Reith, N.A. Straus, Isolation, sequence analysis, and transcriptional studies of the flavodoxin gene from *Anacystis nidulans* R2, J. Bacteriol. 170 (1988) 258–265.
[7] G.N. Hutber, K.G. Hutson, L.J. Rogers, Effect of iron-deficiency on levels of 2 ferredoxins and flavodoxin in a cyanobacterium, FEMS Microbiol. Lett. 1 (1977) 193–196.
[8] N.A. Straus, Iron deprivation: physiology and gene regulation, in: D.A. Bryant (Ed.), The Molecular Biology of Cyanobacteria, Kluwer Academic Publishers, Dordrecht, The Netherlands, 1994, pp. 731–750.
[9] J.W. Murray, J. Duncan, J. Barber, CP43-like chlorophyll binding proteins: structural and evolutionary implications, Trends Plant Sci. 11 (2006) 152–158.
[10] M. Chen, Y. Zhang, R.E. Blankenship, Nomenclature for membrane-bound light-harvesting complexes of cyanobacteria, Photosynth. Res. 95 (2008) 147–154.
[11] J.A. Ihalainen, S. D'Haene, N. Yeremenko, H. van Roon, A.A. Arteni, E.J. Boekema, R. van Grondelle, H.C.P. Matthijs, J.P. Dekker, Aggregates of the chlorophyll-binding protein IsiA (CP43 ′) dissipate energy in cyanobacteria, Biochemistry 44 (2005) 10846–10853.
[12] T.S. Bibby, J. Nield, J. Barber, Iron deficiency induces the formation of an antenna ring around trimeric photosystem I in cyanobacteria, Nature 412 (2001) 743–745.
[13] E.J. Boekema, A. Hifney, A.E. Yakushevska, M. Piotrowski, W. Keegstra, S. Berry, K.P. Michel, E.K. Pistorius, J. Kruip, A giant chlorophyll-protein complex induced by iron deficiency in cyanobacteria, Nature 412 (2001) 745–748.
[14] N. Yeremenko, R. Kouřil, J.A. Ihalainen, S. D'Haene, N. van Oosterwijk, E.G. Andrizhiyevskaya, W. Keegstra, H.L. Dekker, M. Hagemann, E.J. Boekema, H.C.P. Matthijs, J.P. Dekker, Supramolecular organization and dual function of the IsiA chlorophyll-binding protein in cyanobacteria, Biochemistry 43 (2004) 10308–10313.
[15] R. Kouřil, A.A. Arteni, J. Lax, N. Yeremenko, S. D'Haene, M. Rögner, H.C.P. Matthijs, J.P. Dekker, E.J. Boekema, Structure and functional role of supercomplexes of IsiA and photosystem I in cyanobacterial photosynthesis, FEBS Lett. 579 (2005) 3253–3257.
[16] E.G. Andrizhiyevskaya, T.M.E. Schwabe, M. Germano, S. D'Haene, J. Kruip, R. van Grondelle, J.P. Dekker, Spectroscopic properties of PSI–IsiA supercomplexes from the cyanobacterium *Synechococcus* PCC 7942, Biochim. Biophys. Acta Bioenerg. 1556 (2002) 265–272.
[17] E.G. Andrizhiyevskaya, D. Frolov, R. van Grondelle, J.P. Dekker, Energy transfer and trapping in the photosystem I complex of *Synechococcus* PCC 7942 and in its supercomplex with IsiA, Biochim. Biophys. Acta Bioenerg. 1656 (2004) 104–113.
[18] A.N. Melkozernov, T.S. Bibby, S. Lin, J. Barber, R.E. Blankenship, Time-Resolved Absorption and Emission Show that the CP43' Antenna Ring of Iron-Stressed *Synechocystis* sp. PCC6803 Is Efficiently Coupled to the Photosystem I Reaction Center Core, Biochemistry 42 (2003) 3893–3903.
[19] C.D. van der Weij-de Wit, J.A. Ihalainen, E. van de Vijver, S. D'Haene, H.C.P. Matthijs, R. van Grondelle, J.P. Dekker, Fluorescence quenching of IsiA in early stage of iron deficiency and at cryogenic temperatures, Biochim. Biophys. Acta Bioenerg. 1767 (2007) 1393–1400.
[20] S. Sandström, Y.I. Park, G. Öquist, P. Gustafsson, CP43′, the *isiA* gene product, functions as an excitation energy dissipator in the cyanobacterium *Synechococcus* sp. PCC 7942, Photochem. Photobiol. 74 (2001) 431–437.
[21] Y.I. Park, S. Sandström, P. Gustafsson, G. Öquist, Expression of the *isiA* gene is essential for the survival of the cyanobacterium *Synechococcus* sp. PCC 7942 by protecting photosystem II from excess light under iron limitation, Mol. Microbiol. 32 (1999) 123–129.
[22] R. Berera, I.H.M. van Stokkum, S. d'Haene, J.T.M. Kennis, R. van Grondelle, J.P. Dekker, A mechanism of energy dissipation in cyanobacteria, Biophys. J. 96 (2009) 2261–2267.
[23] M. Havaux, G. Guedeney, M. Hagemann, N. Yeremenko, H.C.P. Matthijs, R. Jeanjean, The chlorophyll-binding protein IsiA is inducible by high light and protects the cyanobacterium *Synechocystis* PCC6803 from photooxidative stress, FEBS Lett. 579 (2005) 2289–2293.
[24] J. Vinnemeier, A. Kunert, M. Hagemann, Transcriptional analysis of the *isiAB* operon in salt-stressed cells of the cyanobacterium *Synechocystis* sp. PCC 6803, FEMS Microbiol. Lett. 169 (1998) 323–330.
[25] M. Hagemann, D. Techel, L. Rensing, Comparison of salt-induced and heat-induced alterations of protein synthesis in the cyanobacterium *Synechocystis* sp. PCC 6803, Arch. Microbiol. 155 (1991) 587–592.
[26] T.P.J. Krüger, V.I. Novoderezhkin, C. Ilioaia, R. van Grondelle, Fluorescence spectral dynamics of single LHCII trimers, Biophys. J. 98 (2010) 3093–3101.
[27] R. Berera, C. Herrero, I.H.M. van Stokkum, M. Vengris, G. Kodis, R.E. Palacios, H. van Amerongen, R. van Grondelle, D. Gust, T.A. Moore, A.L. Moore, J.T.M. Kennis, A simple artificial light-harvesting dyad as a model for excess energy dissipation in oxygenic photosynthesis, Proc. Natl. Acad. Sci. U. S. A. 103 (2006) 5343–5348.
[28] A.V. Ruban, R. Berera, C. Ilioaia, I.H.M. van Stokkum, J.T.M. Kennis, A.A. Pascal, H. van Amerongen, B. Robert, P. Horton, R. van Grondelle, Identification of a mechanism of photoprotective energy dissipation in higher plants, Nature 450 (2007) 575–578.
[29] R. Berera, I.H.M. van Stokkum, J.T.M. Kennis, R. van Grondelle, J.P. Dekker, The light-harvesting function of carotenoids in the cyanobacterial stress-inducible IsiA complex, Chem. Phys. 373 (2010) 65–70.
[30] Y. Miloslavina, A. Wehner, P.H. Lambrev, E. Wientjes, M. Reus, G. Garab, R. Croce, A.R. Holzwarth, Far-red fluorescence: a direct spectroscopic marker for LHCII oligomer formation in non-photochemical quenching, FEBS Lett. 582 (2008) 3625–3631.
[31] M.G. Müller, P. Lambrev, M. Reus, E. Wientjes, R. Croce, A.R. Holzwarth, Singlet energy dissipation in the photosystem II light-harvesting complex does Not involve energy transfer to carotenoids, ChemPhysChem 11 (2010) 1289–1296.
[32] M. Wahadoszamen, R. Berera, A.M. Ara, E. Romero, R. van Grondelle, Identification of two emitting sites in the dissipative state of the major light harvesting antenna, Phys. Chem. Chem. Phys. 14 (2012) 759–766.
[33] T. Nakabayashi, M. Wahadoszamen, N. Ohta, External electric field effects on state energy and photoexcitation dynamics of diphenylpolyenes, J. Am. Chem. Soc. 127 (2005) 7041–7052.

[34] A.M. Ara, T. Iimori, T. Yoshizawa, T. Nakabayashi, N. Ohta, External electric field effects on fluorescence of pyrene butyric acid in a polymer film: concentration dependence and temperature dependence, J. Phys. Chem. B 110 (2006) 23669–23677.
[35] L. Premvardhan, E. Papagiannakis, R.G. Hiller, R. van Grondelle, The charge-transfer character of the S-0 → S-2 transition in the carotenoid peridinin is revealed by stark spectroscopy, J. Phys. Chem. B 109 (2005) 15589–15597.
[36] M. Wahadoszamen, A. Ghazaryan, H.E. Cingil, A.M. Ara, C. Buchel, R. van Grondelle, R. Berera, Stark fluorescence spectroscopy reveals two emitting sites in the dissipative state of FCP antennas, Biochim. Biophys. Acta Bioenerg. 1837 (2014) 193–200.
[37] U.K. Laemmli, Cleavage of structural proteins during the assembly of the head of bacteriophage T4, Nature 227 (1970) 680–685.
[38] M. Wahadoszamen, T. Harnada, T. Limori, T. Nakabayashi, N. Ohta, External electric field effects on absorption, fluorescence, and phosphorescence spectra of diphenylpolyynes in a polymer film, J. Phys. Chem. A 111 (2007) 9544–9552.
[39] M. Wahadoszamen, T. Nakabayashi, N. Ohta, External electric field effects on emission of a mixture of tetraphenylporphyrin and fullerene doped in a polymer film, J. Chin. Chem. Soc. 53 (2006) 85–92.
[40] B. Gobets, R. van Grondelle, Energy transfer and trapping in photosystem I, Biochim. Biophys. Acta Bioenerg. 1507 (2001) 80–99.
[41] M. Wahadoszamen, T. Nakabayashi, N. Ohta, Electroabsorption spectra of a complex formed between tetraphenyl-porphyrin and fullerene in a polymer film, J. Photochem. Photobiol. A 178 (2006) 177–184.
[42] T. Polivka, C.A. Kerfeld, T. Pascher, V. Sundstrom, Spectroscopic properties of the carotenoid 3′-hydroxyechinenone in the orange carotenoid protein from the cyanobacterium *Arthrospira* maxima, Biochemistry 44 (2005) 3994–4003.
[43] R. Berera, M. Gwizdala, I.H.M. van Stokkum, D. Kirilovsky, R. van Grondelle, Excited states of the inactive and active forms of the orange carotenoid protein, J. Phys. Chem. B 117 (2013) 9121–9128.
[44] A. Wilson, C. Punginelli, A. Gall, C. Bonetti, M. Alexandre, J.M. Routaboul, C.A. Kerfeld, R. van Grondelle, B. Robert, J.T.M. Kennis, D. Kirilovsky, A photoactive carotenoid protein acting as light intensity sensor, Proc. Natl. Acad. Sci. U. S. A. 105 (2008) 12075–12080.
[45] R. Berera, I.H.M. van Stokkum, M. Gwizdala, A. Wilson, D. Kirilovsky, R. van Grondelle, The photophysics of the orange carotenoid protein, a light-powered molecular switch, J. Phys. Chem. B 116 (2012) 2568–2574.
[46] A. Wilson, G. Ajlani, J.M. Verbavatz, I. Vass, C.A. Kerfeld, D. Kirilovsky, A soluble carotenoid protein involved in phycobilisome-related energy dissipation in cyanobacteria, Plant Cell 18 (2006) 992–1007.